

## Identification of shared genomic aberrations between angiomatous and microcystic meningiomas

Yasuhiro Kuroi, Hiroyuki Akagawa, Makoto Shibuya, Hideaki Onda, Tatsuya Maegawa, and Hidetoshi Kasuya

*Department of Neurosurgery, Tokyo Women's Medical University Medical Center East, Tokyo, Japan (Y.K., H.A., M.S., H.O., T.M., H.K.); Tokyo Women's Medical University, Institute for Integrated Medical Sciences (TIIMS), Tokyo, Japan (Y.K., H.A., T.M., H.K.); Central Laboratory, Hachioji Medical Center, Tokyo Medical University, Tokyo, Japan (M.S.); Division of Neurosurgery, Kofu Neurosurgical Hospital, Kofu, Yamanashi, Japan (H.O.)*

**Corresponding Author:** Hiroyuki Akagawa, MD, Tokyo Women's Medical University, Institute for Integrated Medical Sciences (TIIMS), 8-1 Kawada-cho, Shinjuku-ku, Tokyo, 162-8666 Japan ([akagawa.hiroyuki@twmu.ac.jp](mailto:akagawa.hiroyuki@twmu.ac.jp)).

### Abstract

**Background.** Angiomatous and microcystic meningiomas are classified as rare subtypes of grade I meningiomas by World Health Organization (WHO). They typically exhibit distinct histopathological features as indicated by their WHO titles; however, these angiomatous and microcystic features are often intermixed. Recently, angiomatous meningiomas were reported to show characteristic chromosomal polysomies unlike the other WHO grade I meningiomas. In the present study, we hypothesize that microcystic meningiomas share similar cytogenetic abnormalities with angiomatous meningioma.

**Methods.** We performed copy number analysis using single nucleotide polymorphism (SNP) arrays for three angiomatous and eight microcystic meningiomas. Of these, three angiomatous and three microcystic meningiomas were also analyzed by whole exome sequencing and RNA sequencing.

**Results.** We first analyzed three angiomatous and three microcystic meningiomas for which both frozen tissues and peripheral blood were accessible. Copy number analysis confirmed previously reported multiple polysomies in angiomatous meningiomas, which were entirely replicated in microcystic meningiomas when analyzed on different analytical platforms with five additional samples prepared from formalin-fixed paraffin-embedded tumors. Polysomy of chromosome 5 was found in all cases, along with chromosome 6, 12, 17, 18, and 20 in more than half of the cases including both angiomatous and microcystic meningiomas. Furthermore, next generation sequencing did not reveal any distinctive somatic point mutations or differences in gene expression characterizing either angiomatous or microcystic meningiomas, indicating a common genetic mechanism underlying tumorigenesis.

**Conclusions.** Angiomatous and microcystic meningiomas have substantially similar genetic profiles represented by the characteristic patterns of multiple polysomies originating from chromosome 5 amplification.

### Key Points

- Angiomatous and microcystic meningiomas are hyperdiploid meningiomas.
- Angiomatous and microcystic meningiomas largely share their genetic profiles.
- Chromosome 5 polysomy is a biomarker of angiomatous/microcystic meningiomas.

## Importance of the Study

Current diagnosis of neoplasms incorporates molecular genetic features with the traditional histopathological information. In this study, we hypothesized that microcystic meningiomas share the previously reported cytogenetic abnormalities with angiomatous meningiomas, because of their frequently observed histopathological intermixing. We performed comprehensive genetic analyses in these closely related but different subtypes of meningiomas. The results confirmed that the characteristic multiple polysomies represented by

chromosome 5 amplification in angiomatous meningiomas were entirely replicated in microcystic meningiomas. Furthermore, whole exome and RNA sequencing demonstrated no somatic point mutations or differences in gene expression discriminating angiomatous or microcystic subtypes, indicating a common genetic mechanism underlying tumorigenesis. Chromosome 5 amplification was found in all of the angiomatous/microcystic cases, thereby constituting a potential diagnostic marker and a future therapeutic target.

Meningiomas are the most frequently diagnosed primary brain tumors that account for one-third of all primary brain tumors.<sup>1,2</sup> Most meningiomas (80%) are histologically classified as benign (grade I),<sup>3</sup> which are further subdivided into nine distinct histological variants according to the current World Health Organization (WHO) classifications for meningiomas.<sup>4,5</sup> Among these WHO grade I variants, angiomatous and microcystic meningiomas are distinguished based on the tumor mass consisting either of numerous blood vessels or delicate processes encompassing microcysts, respectively. However, these angiomatous and microcystic features are often intermixed, making it difficult to determine a definitive pathological diagnosis.<sup>5</sup> Such histopathological intermixing also presents a neuroimaging feature resembling high-grade meningiomas based on predisposition to peritumoral brain edema, although angiomatous and microcystic meningiomas do not exhibit aggressive behavior.<sup>4-6</sup>

Recently, angiomatous meningioma was reported to have multiple chromosomal polysomies represented by chromosome 5 amplification, in contrast to most of the other meningiomas having a normal diploid or karyotype with monosomy 22q.<sup>7</sup> In the present study, we hypothesized that microcystic meningioma shares cytogenetic profile similar to angiomatous meningioma. We performed genetic analyses to compare molecular profiles of these closely related but different subtypes of meningiomas.

University Hachioji Medical Center.<sup>4,5</sup> If the tumor contains both angiomatous and microcystic features, it was diagnosed as angiomatous meningioma when vascular components accounted for over 50% of the tumor specimen with reference to the criteria specified by the WHO from 2007.<sup>4</sup> There was no detectable difference in clinical courses between three angiomatous, eight microcystic, and the other 14 typical grade I cases. Of these 25 cases, three angiomatous and three microcystic cases with access to both frozen tissues and peripheral blood samples were subjected to single nucleotide polymorphism (SNP) array, whole exome sequencing (WES), and RNA sequencing (RNA-seq) analysis. The remaining 19 samples were from seven archival formalin-fixed paraffin-embedded (FFPE) tissues including five microcystic cases and 12 frozen tissues from nonangiomatous/microcystic cases (Table 1). These additional samples were used for SNP array analysis. Genomic DNA and total RNA were extracted using standard protocols. This study was approved by the ethics committee of Tokyo Women's Medical University (Approval number: 251C). Relevant informed consent was obtained from subjects.

## Copy Number Analysis Using SNP Array

Genomic DNA samples from six frozen meningiomas and their complementary peripheral leucocytes were hybridized to the Affymetrix Genome Wide Human SNP Array 6.0 (Thermo Fisher Scientific, Waltham, MA). The signal intensity data were processed simultaneously with that of the HapMap individuals ([ftp://ftp.ncbi.nlm.nih.gov/hapmap/raw\\_data/hapmap3\\_affy6.0/](ftp://ftp.ncbi.nlm.nih.gov/hapmap/raw_data/hapmap3_affy6.0/)) using Affymetrix Power Tools (Thermo Fisher Scientific) and the PennCNV-affy package.<sup>8,9</sup> ASCAT 2 was used to calculate somatic copy number profiles from the processed data of B allele frequency (BAF) and Log R ratio (LRR).<sup>10</sup> Control Affymetrix SNP array data consisting of 45 nonangiomatous/microcystic grade I meningiomas was obtained from the previous study by Taberner et al.,<sup>11</sup> which was publicly available in the ArrayExpress database (E-GEOD-42624, <https://www.ebi.ac.uk/arrayexpress/>), and analyzed using the same methods.

## Methods

### Materials

A total of 25 surgically resected cases of meningiomas in our hospital were studied (Table 1). All tumor specimens were submitted to the department of surgical pathology in Tokyo Women's Medical University. Histopathological diagnosis was performed according to the WHO guidelines and double-checked by experienced neuropathologists in collaboration with the central laboratory in Tokyo Medical

**Table 1** Clinicopathological information of studied cases

Sample	Sample type	WHO classification	Sex	Age	Tumor location	Peritumoral edema	Clinical manifestation
AG517	FF*	Angiomatous	M	37	Parasagittal	No	Headache
AG559	FF*	Angiomatous	M	60	Falx	Yes	Headache
AG825	FF*	Angiomatous	M	77	Convexity	Yes	Motor paresis
MC409	FF*, FFPE	Microcystic	F	67	Falx	Yes	Seizure
MC488	FF*	Microcystic	M	64	Convexity	Yes	Seizure
MC505	FF*	Microcystic	F	60	Convexity	No	Motor paresis
MC1	FFPE	Microcystic	M	67	Convexity	No	Asymptomatic
MC2	FFPE	Microcystic	F	58	Convexity	No	Asymptomatic
MC3	FFPE	Microcystic	F	66	Convexity	Yes	Seizure
MC4	FFPE	Microcystic	F	71	Convexity	Unknown	Seizure
MC5	FFPE	Microcystic	F	54	Convexity	Unknown	Unknown
ASA1	FFPE	Meningothelial	F	82	Convexity	Yes	Asymptomatic
ASA2	FFPE	Fibrous	F	48	Falx	No	Dizziness, headache
ASA3	FF	Meningothelial	F	62	Convexity	Yes	Headache, motor paresis
ASA4	FF	Meningothelial	M	63	Convexity	Yes	Unknown
ASA5	FF	Meningothelial	F	70	Convexity	No	Unknown
ASA6	FF	Meningothelial	F	83	Posterior petrous	No	Trigeminal neuralgia
ASA7	FF	Fibrous	F	74	Posterior petrous	No	Asymptomatic
ASA8	FF	Meningothelial	M	75	Convexity	No	Asymptomatic
ASA9	FF	Meningothelial	F	65	Falx	No	Motor paresis
ASA10	FF	Meningothelial	F	67	Parasagittal	Yes	Motor paresis
ASA11	FF	Meningothelial	F	53	Clinoidal	No	Asymptomatic
ASA12	FF	Meningothelial	F	66	Convexity	No	Headache
ASA13	FF	Meningothelial	F	64	Tentorial edge	No	Trigeminal neuralgia
ASA14	FF	Transitional	F	69	Sphenoid ridge	Yes	Asymptomatic

FF = fresh frozen tumor; FFPE = formalin-fixed paraffin-embedded tumor.

\*With peripheral blood sample.

Genomic DNA samples from additional 19 meningiomas without complementary normal tissues were hybridized to the Infinium Asian Screening Array (Illumina, San Diego, CA) to independently verify the results obtained from the Affymetrix array. Processing of the signal intensities and extraction of BAF and LRR data were performed using GenomeStudio 2.0 (Illumina). ASCAT 2 with an option inferring the germline genotypes and GPHMM version 1.3 were used to calculate somatic copy number profiles.<sup>10,12</sup>

GISTIC 2.0 was used to visualize the copy number profiles and to identify regions of the genome that are significantly amplified or deleted across a set of samples.<sup>13</sup>

### Whole Exome Sequencing

Exome capture was performed using SureSelect Human All Exon V5 kit following manufacturer instructions (Agilent Technologies Inc., Santa Clara, CA). Enriched exome libraries were sequenced using 100 bp paired end reads on a HiSeq 2500 sequencer (Illumina). After quality based read trimming, sequence reads were aligned to the human reference genome GRCh37/hg19 using BWA,<sup>14</sup> and duplicate reads marked using the Picard program (<http://broadinstitute.github.io/picard/>). Base substitutions and indels were detected using MuTect2.<sup>15</sup> COSMIC (<https://cancer.sanger.ac.uk/cosmic>), dbSNP (<https://www.ncbi.nlm.nih.gov/snp/>), and a panel of normal variants (<https://gemdbj.ncc.go.jp/omics/docs/others.html>) were used as inputs to MuTect2. Detected somatic mutations were annotated using ANNOVAR,<sup>16</sup> CADD,<sup>17</sup> and FATHMM-Cancer.<sup>18</sup> These were subsequently validated using Sanger method, certified by the following criteria: (i) MuTect2 filter qualification; (ii) Splice site, nonsynonymous, and exonic indel mutations; (iii) variant allele frequencies in tumor samples greater than 0.1; (iv) uncommon variants in general populations; and (v) absence in 16 control exomes using the same exon capture kit and analyzed at the same sequencing center. The Sanger validations were performed via standard PCR-based amplification, followed by BigDye Terminator cycle sequencing on a 3130xl Genetic Analyzer (Thermo Fisher Scientific).

### RNA Sequencing

Libraries were prepared using the TruSeq RNA Sample Preparation Kit v2 (Illumina) according to manufacturer instructions. Each library was paired end sequenced (2 × 75 bp) by using the TruSeq SBS Kit v4-HS, on a HiSeq2500 sequencer (Illumina). RNA-seq transcript data were analyzed using the combination of TopHat2 and Cufflinks.<sup>19</sup> We annotated the assembled transcripts to the UCSC annotation (hg19) obtained from the Illumina iGenomes website ([http://jp.support.illumina.com/sequencing/sequencing\\_software/igenome.html?langsel=jp/](http://jp.support.illumina.com/sequencing/sequencing_software/igenome.html?langsel=jp/)) and used Cufflinks to estimate fragments per kilobase of exon model per million mapped fragments (FPKM). Cufflinks outputs were thoroughly explored and visualized using CummeRbund (<http://compbio.mit.edu/cummeRbund/index.html>).

## Results

We performed comprehensive genetic analyses of three angiomatous and three microcystic meningiomas with access to both frozen tissues and peripheral blood samples (Table 1). Although partial histopathological intermixing was observed in two angiomatous (AG559 and AG825) and one microcystic (MC409) meningiomas (Figure 1), our histopathological diagnosis was clearly supported by low-density appearance of microcystic meningiomas on computed tomography similar to reported characteristics in the literature (Figure 2).<sup>20,21</sup>

Copy number analysis using SNP array (Affymetrix Genome-Wide Human SNP Array 6.0) confirmed previously reported multiple polysomies in angiomatous meningiomas,<sup>7</sup> which was also replicated in microcystic meningiomas (Figure 3). Similar to the previous report,<sup>7</sup> polysomies of chromosome 5 and 6 were found in all six cases, along with chromosome 12, 17, 18, and 20 in more than half of the cases including both angiomatous and microcystic meningiomas (Supplementary Table 1). Angiomatous or microcystic specific copy number alteration was not observed in both chromosomal arm-level and focal gene-level analyses using GISTIC 2.0.<sup>13</sup> These characteristic chromosomal polysomies were not observed in the control Affymetrix SNP array data from 45 other WHO grade I meningiomas in the ArrayExpress database (E-GEOD-42624, <https://www.ebi.ac.uk/arrayexpress/>) (Figure 3).<sup>11</sup> Half of these 45 control meningiomas showed chromosome 22q deletion, reflecting its highest incidence among grade I meningiomas.<sup>2,11</sup> Two out of the six angiomatous/microcystic meningiomas (33.3%) showed chromosome 22q deletion (AG559 and MC488); however, whole exome sequencing (WES) revealed no somatic mutations in *NF2*, supporting a different genetic etiology from many other grade I meningiomas associated with biallelic inactivation of *NF2*.<sup>22</sup> Direct Sanger sequencing confirmed a total of 61 somatic mutations from the WES data (Supplementary Table 2). The major driver genes for non-*NF2* meningioma (*TRAF7*, *KLF4*, *AKT1*, *SMO*, and *POLR2A*) were not mutated, except for AG559 harboring the recurrent p.S561N mutation in *TRAF7* (COSM1578117).<sup>22,23</sup> There were no genes that were commonly mutated in two or more of the angiomatous/microcystic meningiomas. RNA sequencing (RNA-seq) further supported the findings in the SNP array-based copy number analysis and WES, which showed no detectable genomic abnormality discriminating angiomatous and microcystic meningiomas. Density and box plots showing the distribution of RNA-seq read counts (FPKM) equally overlapped one another (Supplementary Figure 1). Hierarchical clustering was inconsistent with the present histopathological diagnosis, forming the closest cluster with the angiomatous AG559 and the microcystic MC488 meningiomas (Supplementary Figure 1). Correlation coefficients of the most distant (MC505 and MC488) and nearest (AG559 and MC488) samples in the hierarchical clusters reached nearly one:  $R^2 = 0.95$  and  $0.98$ , respectively (Supplementary Figure 2). This line of evidences indicates a substantially similar molecular profile of microcystic and angiomatous meningiomas.

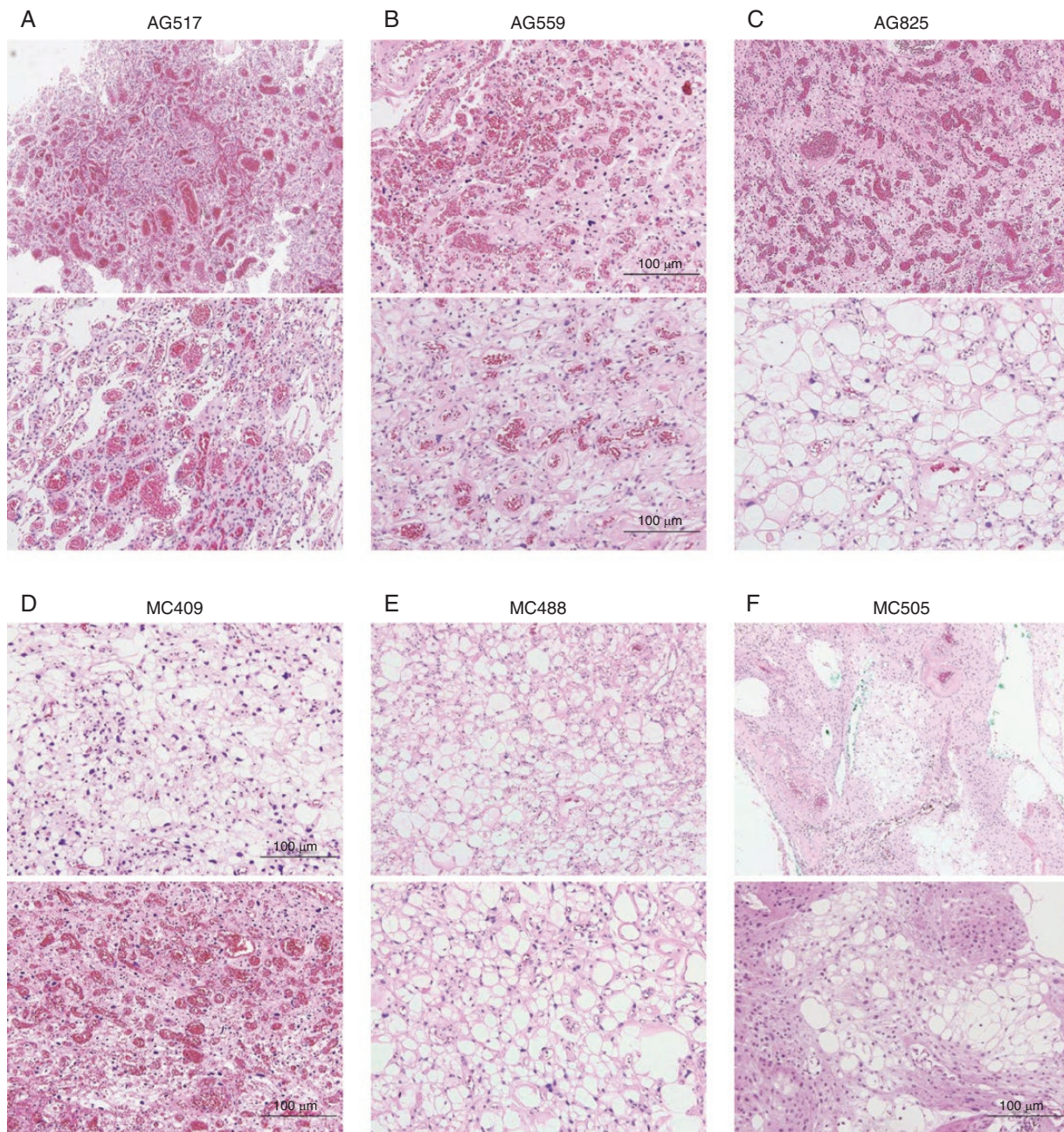


**Figure 1** Histopathological images of six cases of angiomatous and microcystic meningiomas. Hematoxylin and eosin stained sections of angiomatous (a–c) and microcystic (d–f) meningiomas. Representative images providing bases for histopathological diagnosis are shown. Partial histopathological intermixture is observed in (b) AG559, (c) AG825, and (d) MC409 (lower panels).

To further confirm the characteristic multiple polysomies identified in microcystic meningiomas, we added the SNP array based copy number analysis using different types of analytical platforms (Methods). Six microcystic meningiomas whose DNA samples were prepared from FFPE tissues were analyzed using an Illumina BeadChip array (Infinium Asian Screening Array), including MC409 as a positive control (Supplementary Figure 3). Fourteen nonangiomatous/microcystic control samples were from

two FFPE tissues and 12 frozen tissues (Table 1). Copy-number calculations for these additional meningiomas were performed without data from matched normal tissues, which would allow for less cumbersome and cost-effective molecular diagnostics. Although lower resolution due to DNA damage common in FFPE samples, the result of MC409 was entirely replicated as that in the former analysis, and the other microcystic meningiomas also exhibited identical patterns of multiple polysomies

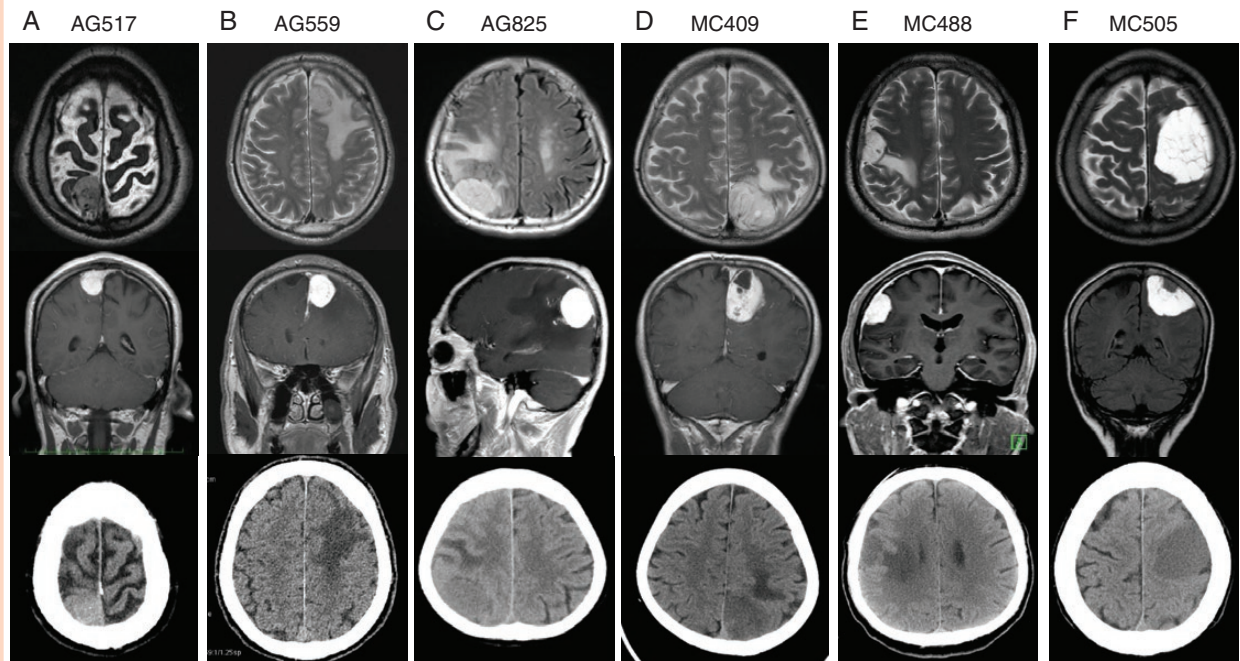


**Figure 2** Radiological images of six cases of angiomatous and microcystic meningiomas. (a–c) are angiomatous, and (d–f) are microcystic meningiomas. T2-weighted magnetic resonance imaging (MRI) of (b–e) shows high-intensity peritumoral edema (upper panels). All tumors show gadolinium enhancement on T1-weighted MRI (middle panels). Microcystic meningiomas (d–f) show low density in computed tomography (lower panels).

represented by chromosome 5 amplification, which were not observed in the 14 nonangiomatous/microcystic control meningiomas (Figure 4).

## Discussion

Microcystic meningioma is a rare histopathological subtype accounting for only 1.6% of all intracranial meningiomas.<sup>20,21</sup> A previous study indicated distinct patterns of hyperdiploidy in this type of meningiomas; Ketter et al.<sup>24</sup> identified 16 hyperdiploid meningiomas from 677 consecutive surgical cases using conventional and fluorescence in situ hybridization-based karyotyping techniques, six of which were WHO grade I meningiomas having microcystic features. However, until the present study, there was no report of genetic analyses using DNA microarrays and next-generation sequencing that focused on microcystic meningiomas. Copy-number analysis confirmed nonrandom patterns of chromosomal polysomies, which were totally identical to that previously reported in angiomatous meningiomas.<sup>7</sup> Chromosome 5, 6, 12, 17, 18, and 20 were frequently amplified, among which amplification of chromosome 5 was found in all of the angiomatous/microcystic cases.<sup>7</sup> In contrast, chromosomal deletions frequently observed in meningiomas at high risk of recurrence, such as 1p, 4p, 6q, 10q, 18q, and 14 losses, were not observed in the present angiomatous/microcystic cases,<sup>25,26</sup> except for MC505 showing monosomy 14

(Figure 3). Careful follow-up is required for cases with these high-risk deletions, such as ASA12 (Figure 4). Next generation sequencing (WES and RNA-seq) further demonstrated no somatic point mutations or differences in gene expression that characterize angiomatous or microcystic meningiomas, indicating a common genetic mechanism in tumorigenesis.

Chromosome instability (CIN), including the multiple polysomies observed in angiomatous/microcystic meningiomas, is one of the major hallmarks of tumor cells; however, the exact mechanisms inducing CIN are not fully understood. Several explanations have been postulated, such as telomere dysfunction and epigenetic alterations.<sup>27,28</sup>

CIN due to telomere fusion is triggered when telomere attrition reaches critical shortening and induces cell apoptosis. However, in many cancer cells, the telomerase reverse transcriptase (*TERT*) gene on chromosome 5p15.33 is upregulated through the promoter hotspot mutations (C228T and C250T) or gene amplification, which lead to both sustained cell proliferation and clonal chromosomal alterations.<sup>29,30</sup> In recent studies, *TERT* promoter mutations were also detected in meningiomas, particularly in higher-grade meningiomas, and were reported to be poor prognostic factors.<sup>5,31</sup> Therefore, it was initially hypothesized that *TERT* activation due to chromosome 5 amplification was potentially responsible for the cytogenetic character of angiomatous/microcystic meningiomas. However, RNA-seq showed no detectable expression of *TERT* (FPKM = 0 in all six tumors), reflecting that the

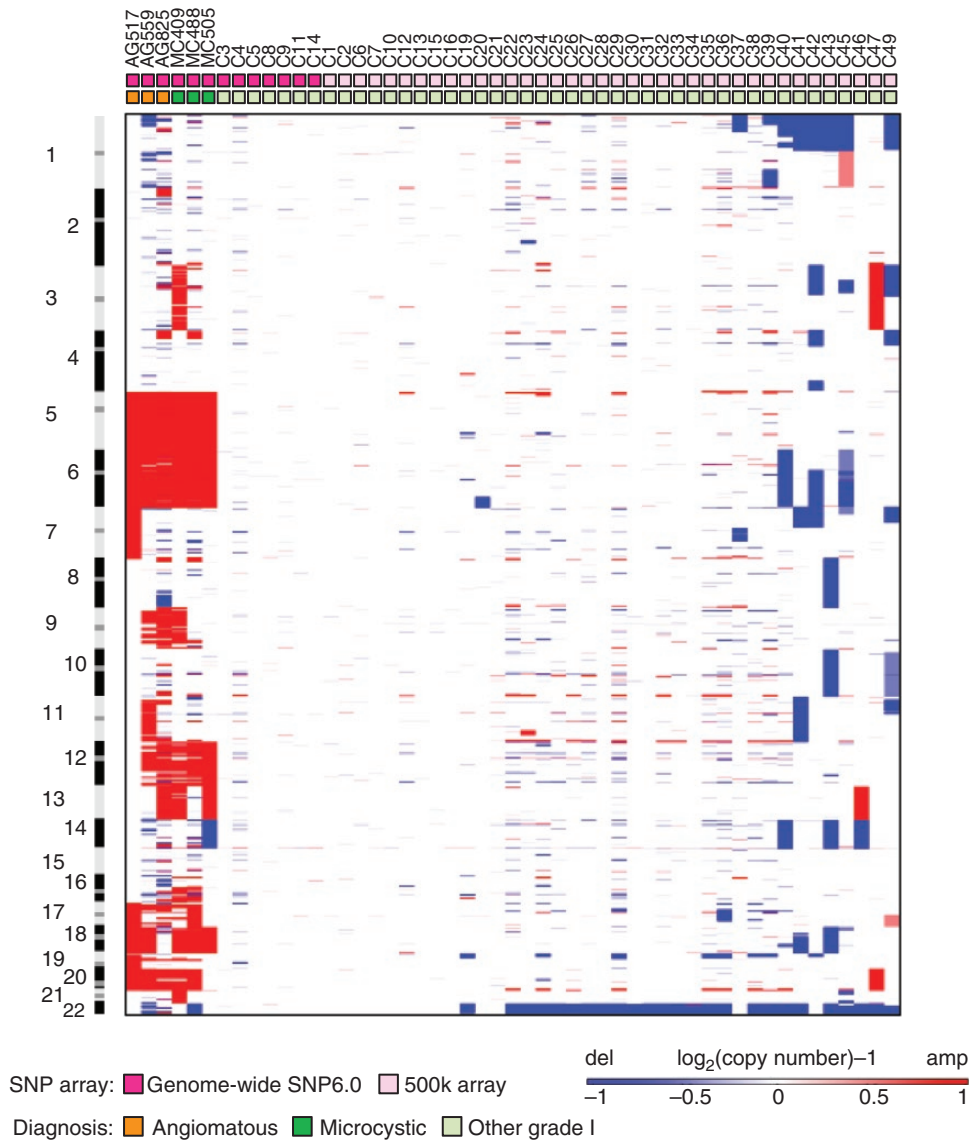


**Figure 3** Copy number profiles calculated using Affymetrix SNP array data. GISTIC 2.0<sup>12</sup> visualizes copy number profiles across the dataset of 51 meningiomas. Of these, 13 including the present six angiomatous/microcystic meningiomas were analyzed by Genome-Wide Human SNP Array 6.0 (red squares) and remaining 38 were by GeneChip Human Mapping 500K array (pink squares). Copy number segmentation was performed using ASCAT 2.<sup>9</sup>

present angiomatous/microcystic cases did not demonstrate aggressive behaviors.

Telomere dysfunction is also implicated in defective DNA double-strand break repair.<sup>32</sup> For example, the *MRE11* gene encoding a double-strand break repair nuclease, which was mutated in the microcystic MC488 meningioma (Supplementary Table 1), plays a central role in double-strand break repair and maintenance of telomere integrity via the MRE11/RAD50/NBS1 complex.<sup>33</sup> Not only somatic mutations,<sup>34,35</sup> but also germline mutations for cancer predisposition were reported in this gene.<sup>36,37</sup> In fact, the p.L473S mutation of *MRE11* (rs771843497) detected in MC488 was reported as a germline mutation in a patient with hereditary breast cancer according to the

ClinVar database (<https://www.ncbi.nlm.nih.gov/clinvar/>). Further investigation is needed because the biological and clinical significance of the p.L473S mutation has not been determined.<sup>37</sup> However, given the nonmalignant nature and the absence of recurrently mutated cancer driver genes among angiomatous/microcystic meningiomas,<sup>7</sup> it was suggested that dosage-balanced genes associated with the frequently amplified chromosomes might confer the tumorigenesis of these hyperdiploid meningiomas rather than somatic driver mutations.<sup>7,24</sup> In this theory, pathogenic hyperdiploidy disrupts stoichiometric balance of gene products forming active multiprotein complexes and pathways associated with cell proliferation signals.<sup>38,39</sup>

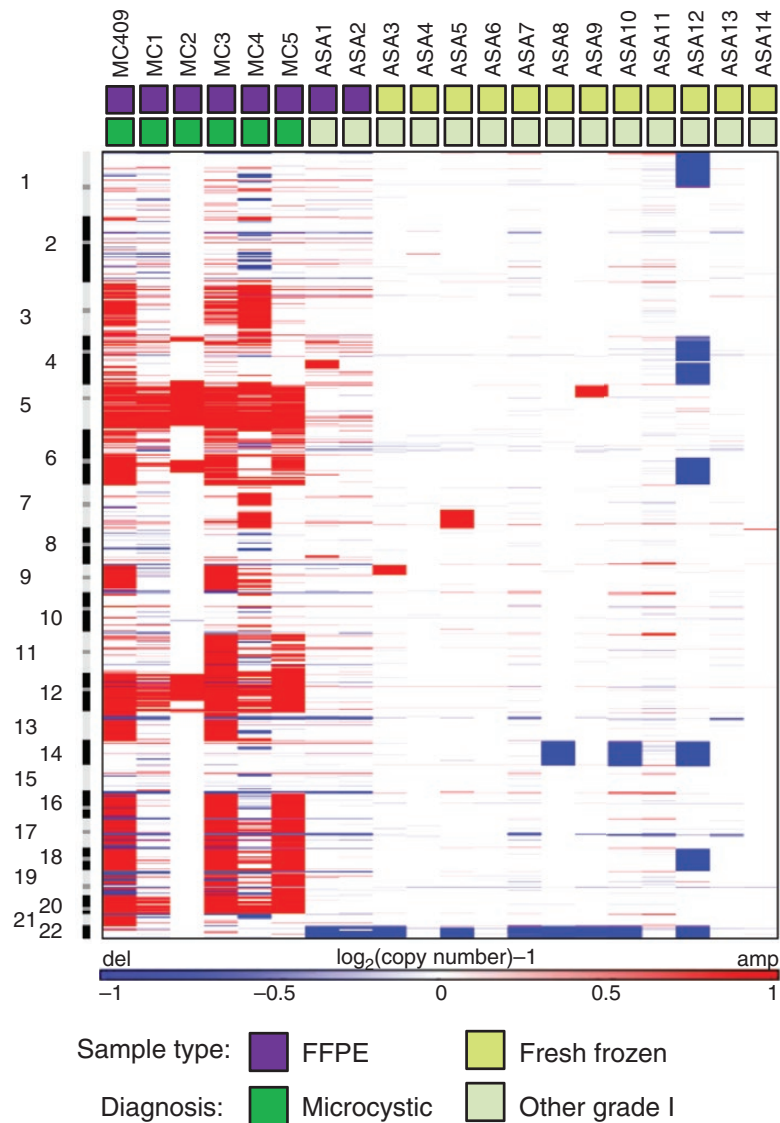


**Figure 4** Copy number profiles calculated using Illumina SNP array data without matched normal samples. GISTIC 2.0<sup>12</sup> visualizes copy number profiles across the dataset of 20 meningiomas, including six microcystic meningiomas from our archival FFPE samples. FFPE = formalin-fixed paraffin-embedded.

Hyperdiploid meningiomas represented by angiomatous meningiomas were reported to have characteristic changes in DNA methylation,<sup>40</sup> which were also known to contribute to CIN.<sup>41</sup> Sahm et al.<sup>40</sup> reported that meningiomas with good postoperative prognosis were clearly subdivided into three classes according to their DNA methylation profiles: the first class denoted as MC-ben-1 was represented by meningiomas with *NF2* loss; the second MC-ben-2 by non-*NF2* meningiomas harboring *TRAF7*, *KLF4*, *AKT1*, or *SMO* mutations; and the third MC-ben-3 by multiple chromosomal gains, most frequently affecting chromosome 5, which include microcystic as well as angiomatous meningiomas. Their analysis further demonstrated that the assignment to these MC-ben-1 to -3 classes had higher power for

predicting good postoperative prognosis than the WHO grading.<sup>40</sup> Although a cause-effect relationship between such DNA methylation changes and hyperdiploidy needs to be clarified, integrated diagnosis using genetic and epigenetic examinations will become increasingly important for clinical decision making in surgical strategies and additional therapeutic options.<sup>25,26,40</sup>

The present study has a few limitations. The number of the samples was limited because of the rarity of angiomatous/microcystic subtypes. Further replication studies with larger sample sizes are required, especially in transcriptome or methylome analysis. Single-cell RNA sequencing, for example, might uncover angiomatous or microcystic specific genetic characteristics that could not be detected by the present bulk tumor analysis. In addition to the comparison between



angiomatous and microcystic subtypes, comparing them with nonhyperdiploid meningiomas is left for future work.

In conclusion, the present study indicated that angiomatous and microcystic meningiomas have substantially similar genetic profiles represented by the characteristic patterns of multiple polysomies originating from chromosome 5 amplification. Although the mechanism underlying such chromosomal aberrations and divergent morphological features needs to be further investigated, polysomy of chromosome 5 can be a promising biomarker providing a novel genetic classification for this angiomatous/microcystic type of meningioma. Dosage-imbalanced genes associated with frequently amplified chromosomes may be potential therapeutic targets for the angiomatous/microcystic meningioma in the future.

## Supplementary Material

Supplementary material is available online at Neuro-Oncology (<http://neuro-oncology.oxfordjournals.org/>).

## Keywords

*Angiomatous meningioma* | microcystic meningioma | copy-number analysis | whole-exome sequencing | RNA sequencing.

## Funding

This work was supported by JSPS KAKENHI (Grant Number 18K16573 [to Y.K.]).

## Acknowledgments

We thank the donors and the supporting medical staff for making this study possible. We also thank Mitsuhiro Amemiya and Akira Saito (StaGen Co. Ltd., Tokyo, Japan) for data processing of next generation sequencing.

## Authorship Statement

M.S., H.O., and H.K. designed the study and H.K. coordinated it. H.K. performed the surgical procedures and provided clinical data and inputs to the project. M.S. performed the histopathological evaluations. Y.K., H.A., M.S., H.O., T.M., and H.K. were involved in the acquisition, analysis, or interpretation of data for the work. Y.K. drafted the manuscript and all other co-authors revised it critically for important intellectual content. All authors have read and approved the final version.

**Conflict of interest statement.** None declared.

## References

1. Wiemels J, Wrensch M, Claus EB. Epidemiology and etiology of meningioma. *J Neurooncol*. 2010;99(3):307–314.
2. Yuzawa S, Nishihara H, Tanaka S. Genetic landscape of meningioma. *Brain Tumor Pathol*. 2016;33(4):237–247.
3. Riemenschneider MJ, Perry A, Reifenberger G. Histological classification and molecular genetics of meningiomas. *Lancet Neurol*. 2006;5(12):1045–1054.
4. Perry A, Louis DL, Scheithauer BW, et al. Meningiomas. In: Louis DN, Ohgaki H, Wiestler OD, et al. eds. *WHO Classification of Tumours of the Central Nervous System*. Lyon: International Agency for Research on Cancer; 2007.
5. Perry A, Louis DN, Budka H, et al. Meningioma. In: Louis DN, Ohgaki H, Wiestler OD, et al. eds. *WHO Classification of Tumours of the Central Nervous System*. Lyon: International Agency for Research on Cancer; 2016.
6. Azizyan A, Eboli P, Drazin D, et al. Differentiation of benign angiomatous and microcystic meningiomas with extensive peritumoral edema from high grade meningiomas with aid of diffusion weighted MRI. *Biomed Res Int*. 2014;2014:650939.
7. Abedalthagafi MS, Merrill PH, Bi WL, et al. Angiomatous meningiomas have a distinct genetic profile with multiple chromosomal polysomies including polysomy of chromosome 5. *Oncotarget*. 2014;5(21):10596–10606.
8. International HapMap Consortium. A haplotype map of the human genome. *Nature*. 2005;437(7063):1299–1320.
9. Wang K, Li M, Hadley D, et al. PennCNV: an integrated hidden Markov model designed for high-resolution copy number variation detection in whole-genome SNP genotyping data. *Genome Res*. 2007;17(11):1665–1674.
10. Van Loo P, Nordgard SH, Lingjærde OC, et al. Allele-specific copy number analysis of tumors. *Proc Natl Acad Sci U S A*. 2010;107(39):16910–16915.
11. Taberner MD, Maíllo A, Nieto AB, et al. Delineation of commonly deleted chromosomal regions in meningiomas by high-density single nucleotide polymorphism genotyping arrays. *Genes Chromosomes Cancer*. 2012;51(6):606–617.
12. Li A, Liu Z, Lezon-Geyda K, et al. GPHMM: an integrated hidden Markov model for identification of copy number alteration and loss of heterozygosity in complex tumor samples using whole genome SNP arrays. *Nucleic Acids Res*. 2011;39(12):4928–4941.
13. Mermel CH, Schumacher SE, Hill B, et al. GISTIC2.0 facilitates sensitive and confident localization of the targets of focal somatic copy-number alteration in human cancers. *Genome Biol*. 2011;12(4):R41.
14. Li H, Durbin R. Fast and accurate short read alignment with Burrows-Wheeler transform. *Bioinformatics*. 2009;25(14):1754–1760.
15. Cibulskis K, Lawrence MS, Carter SL, et al. Sensitive detection of somatic point mutations in impure and heterogeneous cancer samples. *Nat Biotechnol*. 2013;31(3):213–219.
16. Wang K, Li M, Hakonarson H. ANNOVAR: functional annotation of genetic variants from high-throughput sequencing data. *Nucleic Acids Res*. 2010;38(16):e164.
17. Rentzsch P, Witten D, Cooper GM, et al. CADD: predicting the deleteriousness of variants throughout the human genome. *Nucleic Acids Res*. 2019;47(D1):D886–D894.
18. Shihab HA, Gough J, Cooper DN, et al. Predicting the functional consequences of cancer-associated amino acid substitutions. *Bioinformatics*. 2013;29(12):1504–1510.

19. Trapnell C, Roberts A, Goff L, et al. Differential gene and transcript expression analysis of RNA-seq experiments with TopHat and Cufflinks. *Nat Protoc.* 2012;7(3):562–578.
20. Paek SH, Kim SH, Chang KH, et al. Microcystic meningiomas: radiological characteristics of 16 cases. *Acta neurochir (Wien).* 2005;147(9):965–72; discussion 972.
21. Matano F, Adachi K, Murai Y, et al. Microcystic meningioma with late-phase accumulation on thallium-201 single-photon emission computed tomography: case report. *Neurol Med Chir (Tokyo).* 2014;54(8):686–689.
22. Clark VE, Erson-Omay EZ, Serin A, et al. Genomic analysis of non-*NF2* meningiomas reveals mutations in *TRAF7*, *KLF4*, *AKT1*, and *SMO*. *Science.* 2013;339(6123):1077–1080.
23. Clark VE, Harmancı AS, Bai H, et al. Recurrent somatic mutations in *POLR2A* define a distinct subset of meningiomas. *Nat Genet.* 2016;48(10):1253–1259.
24. Ketter R, Kim YJ, Storck S, et al. Hyperdiploidy defines a distinct cytogenetic entity of meningiomas. *J Neurooncol.* 2007;83(2):213–221.
25. Aizer AA, Abedalthagafi M, Bi WL, et al. A prognostic cytogenetic scoring system to guide the adjuvant management of patients with atypical meningioma. *Neuro Oncol.* 2016;18(2):269–274.
26. Nassiri F, Mamatjan Y, Suppiah S, et al. DNA methylation profiling to predict recurrence risk in meningioma: development and validation of a nomogram to optimize clinical management. *Neuro Oncol.* 2019;21:901–910.
27. Vargas-Rondón N, Villegas VE, Rondón-Lagos M. The role of chromosomal instability in cancer and therapeutic responses. *Cancers (Basel).* 2017;10(1):pii:E4.
28. Vajen B, Thomay K, Schlegelberger B. Induction of chromosomal instability via telomere dysfunction and epigenetic alterations in myeloid neoplasia. *Cancers (Basel).* 2013;5(3):857–874.
29. Barthel FP, Wei W, Tang M, et al. Systematic analysis of telomere length and somatic alterations in 31 cancer types. *Nat Genet.* 2017;49(3):349–357.
30. Chiba K, Lorbeer FK, Shain AH, et al. Mutations in the promoter of the telomerase gene *TERT* contribute to tumorigenesis by a two-step mechanism. *Science.* 2017;357(6358):1416–1420.
31. Stögbauer L, Stummer W, Senner V, et al. Telomerase activity, *TERT* expression, hTERT promoter alterations, and alternative lengthening of the telomeres (ALT) in meningiomas - a systematic review. *Neurosurg Rev.* 2019. doi: 10.1007/s10143-019-01087-3.
32. Zhong ZH, Jiang WQ, Cesare AJ, et al. Disruption of telomere maintenance by depletion of the *MRE11/RAD50/NBS1* complex in cells that use alternative lengthening of telomeres. *J Biol Chem.* 2007;282(40):29314–29322.
33. Deng Y, Guo X, Ferguson DO, et al. Multiple roles for *MRE11* at uncapped telomeres. *Nature.* 2009;460(7257):914–918.
34. Sjöblom T, Jones S, Wood LD, et al. The consensus coding sequences of human breast and colorectal cancers. *Science.* 2006;314(5797):268–274.
35. Fukuda T, Sumiyoshi T, Takahashi M, et al. Alterations of the double-strand break repair gene *MRE11* in cancer. *Cancer Res.* 2001;61(1):23–26.
36. Regal JA, Festerling TA, Buis JM, et al. Disease-associated *MRE11* mutants impact ATM/ATR DNA damage signaling by distinct mechanisms. *Hum Mol Genet.* 2013;22(25):5146–5159.
37. Kim H, Cho DY, Choi DH, et al. Frequency of pathogenic germline mutation in *CHEK2*, *PALB2*, *MRE11*, and *RAD50* in patients at high risk for hereditary breast cancer. *Breast Cancer Res Treat.* 2017;161(1):95–102.
38. Birchler JA, Veitia RA. Gene balance hypothesis: connecting issues of dosage sensitivity across biological disciplines. *Proc Natl Acad Sci U S A.* 2012;109(37):14746–14753.
39. Rice AM, McLysaght A. Dosage-sensitive genes in evolution and disease. *BMC Biol.* 2017;15(1):78.
40. Sahn F, Schrimpf D, Stichel D, et al. DNA methylation-based classification and grading system for meningioma: a multicentre, retrospective analysis. *Lancet Oncol.* 2017;18(5):682–694.
41. Herrera LA, Prada D, Andonegui MA, et al. The epigenetic origin of aneuploidy. *Curr Genomics.* 2008;9(1):43–50.